

Fast Planar Correlation Clustering for Image Segmentation

Julian Yarkony, Alexander Ihler, Charless C. Fowlkes
{jyarkony, ihler, fowlkes}@ics.uci.edu

Department of Computer Science, University of California, Irvine

Abstract. We describe a new optimization scheme for finding high-quality clusterings in planar graphs that uses weighted perfect matching as a subroutine. Our method provides lower-bounds on the energy of the optimal correlation clustering that are typically fast to compute and tight in practice. We demonstrate our algorithm on the problem of image segmentation where this approach outperforms existing global optimization techniques in minimizing the objective and is competitive with the state of the art in producing high-quality segmentations.¹

1 Introduction

We tackle the problem of generic image segmentation where the goal is to partition the pixels of an image into sets corresponding to objects and surfaces in a scene. Cues for this task can come from both bottom-up (e.g., local edge contrast) and top-down (e.g., recognition of familiar objects). For closed domains where top-down information is available, this problem can be phrased in terms of labeling each pixel with one of several category labels or perhaps “background”. There is a rapidly developing body of research in this area that integrates multiple cues such as the output of a bank of object detectors into a single model, typically formulated as a Markov random field over the pixel labels and some additional hidden variables [1,2,3,4,5,6,7].

When top-down information is not available, it may still be quite valuable to estimate image segments. Bottom-up segmentations provide candidate support for novel objects and can simplify the processing of the scene to the problem of understanding a small number of salient regions. Without a predefined set of labels, it is natural to describe the segmentation task as a graph partitioning problem in which pixels or superpixels have pairwise or higher order similarities and the number of parts must be estimated. There is a rich history of applying graph partitioning techniques to image segmentation (e.g., [8,9,10,11,12]).

Here we consider the weighted correlation clustering objective which sums up the edges cut by a proposed partitioning of the graph. Edges may have both positive and negative weights. Correlation clustering is appealing since the optimal number of segments emerges naturally as a function of the edge weights

¹ This is the extended version of a paper to appear at the 12th European Conference on Computer Vision (ECCV 2012)

rather than requiring an additional search over some model order parameter. Further, because the objective is linear in the edge weights, the problem of learning can be approached using techniques from structured prediction [13].

As with many non-trivial graph partitioning criteria, finding a minimum weight correlation clustering is NP-hard for general graphs [14]. Demaine et al. [15] provide results on the hardness of approximation in general graphs by reduction to/from multiway cut [16]. Recently, Bachrach et al. [17] also showed that correlation clustering is NP-hard in planar graphs by a reduction from planar independent set.

Despite these difficulties, correlation clustering has seen a few recent applications to the image segmentation problem. Andres et al. [18] define a model for image segmentation that scores segmentations based on the sum of costs associated with each edge in the segmentation and optimize it using an integer linear programming (ILP) branch-and-cut strategy. Kim et al. [19] use a correlation clustering model for segmentation which includes higher-order potentials or hyper-edges that define cost over sets of nodes which they solve using linear programming (LP) relaxation techniques.

In this paper, we describe a new optimization strategy that specifically exploits the planar structure of the image graph. Our approach uses weighted perfect matching to find candidate cuts in re-weighted versions of the original graph and then combines these cuts into a final clustering. The collection of cuts form constraints in a linear program that lower-bounds the energy of the true correlation clustering. In practice this lower-bound and the cost of the output clustering are almost always equal, yielding a certificate of global optimality. We compare this new optimization scheme to existing approaches based on both standard LP relaxations and ILP and find that our approach is substantially faster and provides tighter lower-bounds for a wide range of image segmentation problems.

2 Correlation Clustering

Correlation clustering is a clustering criteria based on pairwise (dis)similarities. Let $G = (V, E)$ be an undirected graph with edge weights $\theta_e \in \mathbb{R}$ that specify the similarity or dissimilarity on an edge $e = (i, j)$ between vertices i and j . Correlation clustering seeks a clustering of the vertices into disjoint sets $V = V_1 \sqcup V_2 \sqcup V_3 \dots$ that minimizes the total weight of edges between clusters.²

Let X_e be a binary indicator variable specifying which edges are “cut” by the partitioning. $X_e = 0$ if edge $e = (u, v)$ is within a cluster (i.e., $u, v \in V_i$) and $X_e = 1$ if e runs between two clusters (i.e., $u \in V_i, v \in V_j, i \neq j$). Let \mathcal{C} indicate the configurations of X that correspond to valid partitionings of the vertices. We can describe this succinctly by the set of triangle inequalities

$$\mathcal{C} = \{X : X_{u,w} + X_{w,v} \geq X_{u,v} \quad \forall u, v, w \in V\}$$

² This objective is equivalent (up to a constant) with the minimum-disagreement or maximum-agreement objectives mentioned in the literature [14,15].

These constraints enforce transitivity of the clustering; if edge (u, w) is cut, then at least one of (u, w) and (w, v) must also be cut.

We can express the correlation clustering problem as:

$$CC^* = \min_{X \in \mathcal{C}} \sum_{e \in E} \theta_e X_e$$

and refer to CC^* as the cost or the energy of the optimal clustering. Where appropriate, we will use $CC^*(\theta)$ to indicate the dependence of this optimum on the parameters.

Unlike other graph partitioning objectives (min-cut, normalized-cut, etc.) the edge weights can be both positive and negative. Furthermore, we do not specify the number of segments *a priori* or place any constraints on their size. Instead, these arise naturally from the edge weights. For example, if all the edge weights are negative, each vertex will be placed in a separate cluster. If all the edge weights are positive, the optimal solution is to place all vertices in a single cluster. This means that CC^* is upper-bounded by 0 since placing all the vertices in the same cluster is a valid partitioning with cost 0.

The correlation clustering objective appears very similar to standard pairwise Markov Random Field (MRF) models for image labeling. For example, if we knew the optimal solution consisted of k clusters, we could convert the problem into a k -state MRF without any unary terms. In the next section we make this connection precise.

3 Clusterings and Colorings

Consider a partitioning of the graph represented by $X \in \mathcal{C}$. We call this partitioning *k-colorable* if there is some labeling $L : V \rightarrow 1, 2, \dots, k$ of the vertices of the graph so that $X_{uv} = 1 \Leftrightarrow L(u) \neq L(v)$. For every graph, there is a minimal number of colors $\gamma(G)$, known as the *chromatic number* of G , that is sufficient to represent all partitions. Let \mathcal{C}_k be the set of partitionings that are representable by k colors, then $\mathcal{C}_1 \subset \mathcal{C}_2 \subset \dots \subset \mathcal{C}_{\gamma(G)} = \mathcal{C}$. For example, the four-color theorem [20] shows that any partition of a planar graph can be represented by $k = 4$ labels so $\mathcal{C} = \mathcal{C}_4$ for planar graphs.

This provides a useful alternative formulation of correlation clustering in terms of vertex labels. Let $L_v \in 1, \dots, k$ be a label variable for vertex v . Then we can define an equivalent optimization problem

$$CC_k^* = \min_{L \in \{1, \dots, k\}^N} \sum_{(u,v) \in E} \theta_{u,v} [L_u \neq L_v]$$

To produce a partitioning from the labeling, simply take the collection of connected components for the subgraph induced by each label in turn. If G is k -colorable, then $CC_q^* = CC^*$ for any $q \geq k$. In general $CC_q^* \geq CC^*$ for $q < k$ since the optimal partitioning of G may not be q -colorable. The set of 2-colorable partitions are commonly referred to as cuts of a graph.

Since planar graphs are 4-colorable, $CC^* = CC_4^*$. We could tackle the problem planar correlation clustering using the standard set of tools for optimizing a 4-state MRF with mixed (attractive/repulsive) potentials. Since the combinatorial optimization is NP hard, such methods can only give approximate solutions. Furthermore, many of them perform poorly on problems with no unary potentials. Since the energy function is symmetric with respect to permutations of the labels, the true max-marginals for the node labels are uninformative and one is forced to look at higher-order constraints. For example, the lower-bound provided by TRW [21,22] is simply the sum of the negative edge weights in the graph.

One interesting exception is the case of planar binary labeling problems. For planar graphs, the cost of the optimal binary labeling CC_2^* can be computed by an efficient reduction to weighted perfect matching in a suitably augmented planar dual of the graph G . This idea was first described in the statistical physics literature by Kasteleyn [23] and Fisher [24] in the context of computing the partition function of an Ising model. Recently, this has been explored as a tool for finding MAP configurations of more general MRFs that include an external field [25,26,27,28,29].

Since 2-colorable partitions are a subset of 4-colorable partitions, finding the optimal 2-colorable partitioning does not necessarily give us the optimal clustering of a planar graph. The space of 4-colorable partitions is larger so in general $CC_2^* \geq CC_4^*$. However, the optimal 2-coloring still provides some useful information about the optimal 4-colorable partition.

Proposition 1. *For any graph, $0 \geq CC_2^* \geq CC_4^* \geq \frac{3}{2}CC_2^*$ so the cost of the optimal planar correlation clustering is bounded below by $\frac{3}{2}$ the cost of the optimal 2-colorable partition.*

Proof. For a partitioning described by some labeling L , let

$$S(a, b) = \sum_{\substack{u:L_u=a \\ v:L_v=b}} \theta_{u,v}$$

denote the sum of weights of edges between vertices labeled a and those labeled b . Take the 4-colorable partition whose cost is $CC_4^* = \sum_{a < b} S(a, b)$ and consider the 2-colorable partitions in which pairs of labels from the 4-coloring are merged. There are three such 2-colorings, each with the following costs

$$E_a = S(1, 3) + S(1, 4) + S(2, 3) + S(2, 4) \tag{1}$$

$$E_b = S(1, 2) + S(1, 4) + S(3, 2) + S(3, 4) \tag{2}$$

$$E_c = S(1, 2) + S(1, 3) + S(4, 2) + S(4, 3) \tag{3}$$

Summing these costs includes every possible S term twice so we have

$$CC_4^* = \frac{1}{2}(E_a + E_b + E_c) \quad (4)$$

$$\geq \frac{3}{2} \min\{E_a, E_b, E_c\} \quad (5)$$

$$\geq \frac{3}{2} CC_2^* \quad (6)$$

The first inequality follows since one of the three terms in the sum must be at least as small as $1/3$ the total. The second inequality follows since none of these 2-colorings can have lower cost than the optimum 2-coloring. The same approach can be used to relate any pair of CC_m^* and CC_n^* .

Corollary 1. *If $CC_2^* = 0$ then $CC_4^* = 0$.*

Since the 2-colorable clustering is only off by a constant factor and provides a very efficient solution for finding approximate correlation clusterings, it seems a likely candidate for segmentation. However, in practice, it performs poorly for real image segmentation problems. In natural images, T-junctions where three different image segments come together are common, and such a junction cannot be 2-colored! In the next section, we devise a tighter bound which uses the 2-coloring as a subroutine.

4 Lower-bounding Planar Correlation Clustering

Dual-decomposition provides a very general framework for tackling difficult problems by splitting them into a collection of tractable sub-problems which are solved independently subject to the constraint that they agree on their solutions. This constraint is enforced in a soft way using Lagrange multipliers, which results in a dual solution that lower-bounds the original minimization problem. Decomposition techniques have been studied in the optimization community for decades. Dual-decomposition was used by Wainwright et al. [21] to derive algorithms for inference in graphical models and has become increasingly popular in the computer vision literature recently due to its flexibility [30].

We consider bounding the planar correlation clustering by a decomposition into two sub-problems, an easier partitioning problem and an independent edge problem that does not enforce the clustering constraints. To make the partitioning problem tractable, we impose a constraint on the decomposition so that the cost of the optimal clustering can be computed. Recall our notation that $CC^*(\lambda)$ is the optimal correlation clustering cost associated with edge weights λ . Let the set $\Omega = \{\lambda : CC^*(\lambda) = 0\}$ be those those edges weights for which the optimal clustering has zero cost. We can then write the following decomposition bound:

$$CC^* = \min_{X \in \mathcal{C}_4} \sum_{e \in E} \theta_e X_e \quad (7)$$

$$= \max_{\lambda} \left(\min_{\hat{X} \in \mathcal{C}_4} \sum_{e \in E} \lambda_e \hat{X}_e \right) + \left(\min_{\bar{X}} \sum_{e \in E} (\theta_e - \lambda_e) \bar{X}_e \right) \quad (8)$$

$$\geq \max_{\lambda \in \Omega} \left(\min_{\hat{X} \in \mathcal{C}_4} \sum_{e \in E} \lambda_e \hat{X}_e \right) + \left(\min_{\bar{X}} \sum_{e \in E} (\theta_e - \lambda_e) \bar{X}_e \right) \quad (9)$$

$$= \max_{\lambda \in \Omega} \left(\min_{\bar{X}} \sum_{e \in E} (\theta_e - \lambda_e) \bar{X}_e \right) \quad (10)$$

$$= \max_{\lambda \in \Omega} \sum_{e \in E} \min\{(\theta_e - \lambda_e), 0\} \quad (11)$$

In equation (8) we have decomposed the original edge weights θ across two sub-problems. The first is a correlation clustering problem (identical in form to our original problem) while the second one independently optimizes over all the edges (with no constraints on X). For any choice of λ , these two objectives sum up to the original problem. Since the configurations (\hat{X}, \bar{X}) in each sub-problem are optimized independently, the sum of their energies may produce a lower-bound for arbitrary λ but the bound can be made tight (setting $\lambda_e = \theta_e$ recovers the original objective). In equation (9), we restrict the domain of λ to those settings for which the clustering sub-problem has an optimum of zero. The inequality arises since we are maximizing the bound over a more restrictive set. Finally, in equation (10) we have simplified the expression since the constraint on λ entails that the first term is exactly zero and \bar{X} can be optimized independently for each edge.

5 Bound Optimization using Linear Programming

Lagrangian relaxation approaches typically use projected sub-gradient ascent or other non-smooth optimization techniques to tackle objectives like that shown in equation (9). Here it is difficult to compute the required (sub)gradient information since, for a given setting of λ , there isn't an obvious way to recover the full set of optimizing solutions for \hat{X} beyond the trivial solution $\hat{X}_e = 0$. The constraint set Ω also appears quite complicated. However, we do have an efficient method for testing membership in Ω . By our earlier proposition,

$$\Omega = \{\lambda : CC^*(\lambda) = 0\} = \{\lambda : CC_2^*(\lambda) = 0\} \quad (12)$$

$$= \{\lambda : \sum_e \lambda_e X_e \geq 0 \quad \forall X \in \mathcal{C}_2\} \quad (13)$$

This expression highlights that Ω is a polytope defined by a set of linear inequalities. For a given λ , we can test membership and, if $\lambda \notin \Omega$, produce a violated

constraint described by a negative weight 2-colorable clustering. This provides a method to solve equation (11) using cutting planes to successively approximate the constraint set Ω .

We say that an edge e is *constrained* by Ω for a given setting of λ if there exists some cut in $X \in \mathcal{C}_2$ with $X_e = 1$ and for which $\sum_e \lambda_e X_e = 0$. If an edge e is unconstrained, then we can decrease λ_e and thereby increase the bound until it becomes constrained or until it is no longer cut in the independent edge problem.

To simplify the bound optimization, we first consider some additional constraints on λ . When maximizing the bound over λ_e , it is always the case that there is an optimal $\lambda_e \geq \theta_e$. Choosing $\lambda_e < \theta_e$ gives the edge e positive weight in the independent edge problem so it does nothing to increase the objective. Further, any amount by which λ_e is less than θ_e can only make the constraints Ω more difficult to satisfy. Therefore, we are free to only consider λ for which $(\theta_e - \lambda_e) \leq 0$ without impacting the final bound. This simplifies the expression for the objective in equation (11) by removing the min.

We also impose upper bounds on λ . For edges with $\theta_e < 0$ we add the constraint that $\lambda_e \leq 0$. For edges with $\theta_e \geq 0$ we impose the constraint that $\lambda_e = \theta_e$. These constraints are sensible in that they are coordinate-wise optimal (e.g., increasing λ_e above $\theta_e \geq 0$ decreases the bound). In Appendix B, we show that any optimal λ can be deformed to one which satisfies these additional constraints without loosening the bound. In practice these additional constraints make the bound optimization far more efficient.

We can now write the bound optimization problem with these additional constraints explicitly as standard linear program:

$$\begin{aligned} \max_{\lambda} \quad & \sum_e (\theta_e - \lambda_e) & (14) \\ \text{s.t.} \quad & \theta_e \leq \lambda_e \leq \max\{0, \theta_e\} \\ & \sum_e \lambda_e X_e \geq 0 \quad \forall X \in \mathcal{C}_2 \end{aligned}$$

This LP has an exponential number of constraints, one for every possible 2-colorable partition X . To solve this LP efficiently, we use a cutting plane approach to successively add violated constraints to a collection. Our final algorithm for bound optimization is given in Figure 1.

In our actual implementation, we perform one additional step. Each new constraint X may partition the graph into multiple components. We break the cut X up into the set of basic cuts, each of which isolates a component. We add this collection of constraints as a batch. With this modification, we find that in practice very few batches of constraints (typically 5-10) are necessary in order to produce a solution to the full linear program.

Lower-bound optimization	Upper-bound decoding
$\mathcal{P} = \emptyset$	$S = 0$
while $CC_2^*(\lambda) < 0$ do	$\mathcal{E} = \{e : \theta_e - \lambda_e < 0\}$
$X = \arg \min_{X \in \mathcal{C}_2} \sum_{e \in E} \lambda_e X_e$	for $e \in \mathcal{E}$ do
$\mathcal{P} = \mathcal{P} \cup X$	$X = \arg \min_{X \in \mathcal{C}_2, X_e=1} \sum_{f \in E} \lambda_f X_f$
Solve (14) with partial constraint	$S' = \max(S, X)$
set $\mathcal{P} \subset \mathcal{C}_2$	if $\sum_e \theta_e S'_e \leq \sum_e \theta_e S_e$ then
end while	$S = S'$
	$\forall e : X_e = 1, \lambda_e = 0$
	end if
	end for

Fig. 1. (left) Cutting plane algorithm for computing the optimal lower-bound by successively adding constraints. (right) Upper-bound decoding by recursive partitioning

6 Decoding upper-bounds

6.1 Recursive Bipartitioning

Once we have optimized the lower-bound, we would like to find a corresponding low-cost clustering. In general, there will be some edges for which $(\theta_e - \lambda_e) < 0$. In order for the bound to be tight, we need to find a clustering in which these edges are cut. As noted in the previous section, every such “must cut” edge is constrained by some cut \hat{X} that includes that edge. Although none of the individual minimal cuts \hat{X} may agree with all of the “must cut” edges in the independent sub-problem (second term in equation (9)), there is some minimal cut that agrees with each one.

Motivated by this intuition, one can use the following decoding technique. Start with the original clustering sub-problem which has edge weights λ . Choose an ordering of those edges e for which $(\theta_e - \lambda_e) < 0$. For each of these “must cut” edges in turn, find a zero weight cut $X \in \mathcal{C}_2$ for the clustering subproblem and add it to the final partitioning as long as it decreases the original objective. Remove these cut edges from the graph and continue on with the next edge. The pseudo-code is displayed in Figure 1.

6.2 Dual LP Rounding

An alternative approach is to consider the dual LP to equation (14). Let C be a matrix whose rows contain the indicator vectors for cuts $X \in \mathcal{C}$. Define the convex cone $\mathcal{C}_2^\Delta = \{C^T \alpha, \alpha \geq 0\}$ which is known as the “cut cone” [31]. It is straightforward to see that the set of valid partitions lives inside the cut cone ($\mathcal{C} \subset \mathcal{C}_2^\Delta$). Given a valid partition indicator vector X , we can write it as a linear combination of cuts, where each cut isolates an individual segment and the cuts are assigned a weight of $\alpha_i = 0.5$.

The dual LP to our lower-bound is given by

$$\begin{aligned} \min_z \theta^T z - \min(\theta^T, 0) \max(z - 1, 0) \\ \text{s.t. } z \in \mathcal{C}_2^\Delta \end{aligned} \quad (15)$$

The first term in the objective is exactly our original correlation clustering objective where the binary indicator X has been replaced by real valued z . The second term in the objective arises from the upper-bound constraints imposed on λ and effectively cancels out the benefit of cutting any negative weight edge by an amount of more than one (see Appendix A). To compute a solution to the dual, we solve (15) using a matrix C that contains only those cut vectors in \mathcal{P} produced during the lower-bound optimization. The resulting solution vector z is thresholded to produce a final segmentation.

Taking the dual of equation (14) without the upper-bound constraints on λ yields a nice interpretation of our algorithm as a convex relaxation of the original discrete clustering problem in which the convex hull of \mathcal{C} is approximated by the intersection of the cut cone and the unit cube:

$$\min_z \theta^T z \quad \text{s.t. } z \in \mathcal{C}_2^\Delta, \quad 0 \leq z \leq 1 \quad (16)$$

Since the cut cone for planar graphs can be described with a polynomial number of constraints [32], one could directly solve the dual LP in equation (16). Our bound optimization gains considerable efficiency by not using the full set of cuts C . Instead, a small number of cutting planes (in the original LP) provides a delayed column generation scheme for solving the dual LP.

When only using a subset of cuts, the second term in (15) and the corresponding constraints in the primal LP are necessary since the bound can be tight without the optimal partition vector living in the subspace of the cut cone described by \mathcal{P} . Allowing solutions with $z > 1$ lets us access a larger set partitions without increasing the dimensionality of the subspace.

7 Experiments

We demonstrate the performance of our algorithm on correlation clustering problem instances from the Berkeley Segmentation Data set [33,34]. Our clustering problem is defined on the superpixel graph given by performing the oriented watershed transform (owt) on the output of the “generalized probability of boundary” (gPb) boundary detector output as proposed by [34]. Each pair of superpixels that are adjacent in the image are connected by an edge whose weight is given by

$$\theta_e = \log \left(\frac{1 - gPb_e}{gPb_e} \right) + \beta$$

where gPb_e is the average gPb along the edge and β is a threshold parameter that modulates the number of segments in the optimal clustering. Large β results

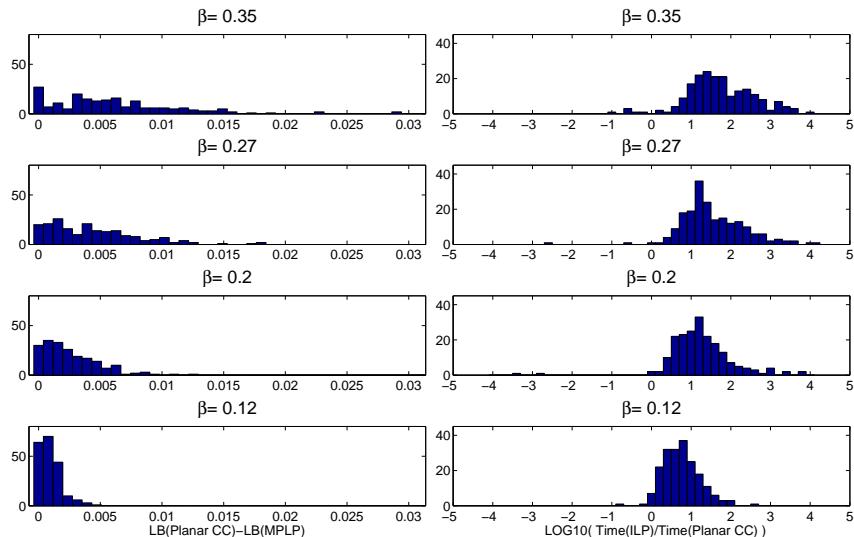


Fig. 2. Comparison of bound optimization on image segmentation problems. Each graph shows the distribution results over 200 problem instances at four different threshold settings ranging from coarse ($\beta = 0.35$) to fine ($\beta = 0.12$). The left column shows the difference in the lower-bounds returned by the PlanarCC bound and MPLP using the set of face cycle constraints. Our code returned tight bounds in all but one instance while the LP relaxation typically gave looser bounds. The right column shows the running times of our approach compared to the ILP branch-and-cut advocated by [18]. Here we plot relative speedup factors on a logarithmic scale. We find that the PlanarCC bound computation and decoding produces the same global optima as the ILP approach much faster.

in more positive edges and hence coarser optimal segmentations. To compare different optimizers, we use 4 different settings of $\beta = \{0.35, 0.27, 0.20, 0.12\}$ which produces segmentation outputs that cover a range of granularities. Parameters θ were rounded to 5 decimal places in order to simplify tests of convergence.

We implemented our optimization using the BlossomV minimum weight perfect matching code [35,36] and IBM’s CPLEX solver to optimize the lower-bound. We used a tolerance of -10^{-6} as a stopping criterion for adding additional constraints to the lower-bound LP. We found that both decoding schemes work well. In the experiments described here, we computed up to ten upper bounds using the recursive bipartitioning procedure, each run using a random order for adding contours. This process terminated early if the lower- and upper-bounds were equal.

For a baseline lower-bounding scheme, we used max-product linear programming (MPLP) [37] which efficiently solves an LP relaxation of the original clus-

tering objective. To represent the set of clusterings in terms of node labels, each superpixel takes on one of 4 states and pairwise potentials encode the boundary strength between neighboring superpixels. As mentioned before, the standard edge-based relaxation is uninformative when unary potentials are absent so we include the set of cycle constraints given by collection of cycles that bound the planar faces of the superpixel graph. This is not sufficient to enforce consistency over all cycles in the graph but is a natural choice commonly used in the literature. In our experiments, we used a fast, in-house implementation of MPLP.

We also implemented the branch-and-cut ILP technique proposed by [18] using the CPLEX ILP solver. This approach finds an integral solution of the correlation clustering objective, removes cut edges specified in the solution and then produces a partition by finding connected components of the resulting graph. It then searches for inconsistent edges, namely cut edges that connect two nodes that lie within the same connected component. If any such edges are found, a constraint is added to enforce consistency of that edge and the ILP is re-solved.

7.1 Bound optimization experiments

Figure 2 shows a comparison of the lower-bounds generated by MPLP compared to that generated by PlanarCC. We found that the time needed for MPLP to solve each problem is comparable to that of PlanarCC. However the differences in the lower-bound are significant. With only the set of face cycles, MPLP is seldom able to produce a tight lower-bound. In contrast, the PlanarCC approach typically gives tight bounds with only 5-10 batches of cut constraints.

We found that the upper-bounds (solutions) generated by ILP and PlanarCC are very similar and very close to optimal so we compare the time consumed by each algorithm as a function of β . In Figure 2(a) we show histogram of the comparative run times, $\log_{10}(T_{ILP}/T_{PlanarCC})$.

Note that the relative performance of PlanarCC improves as we move from a high detail segmentation $\beta = 0.12$ to a coarse segmentation $\beta = 0.35$. For coarse segmentations (large β) the optimal solution contains many long contours and PlanarCC performs well relative to ILP, whereas for detailed segmentations ILP will tend to do more favorably. For example, in the limit where all the edges have negative weight, the ILP approach or LP relaxation gives the correct answer (cut all edges) without the need for any constraints. However on average, we find that the PlanarCC approach performs favorably across a range of useful thresholds on the BSDS images, giving speedups that range from 10 to 1000x.

7.2 Segmentation performance

We benchmark the quality of the segmentations produced by correlation clustering for a range of thresholds β on the BSDS500 test set. We use the same superpixels and local cues as the top performing gPb+owt+UCM algorithm of Arbelaez et al. [34]. Figure 3 shows the benchmark results of our algorithm and

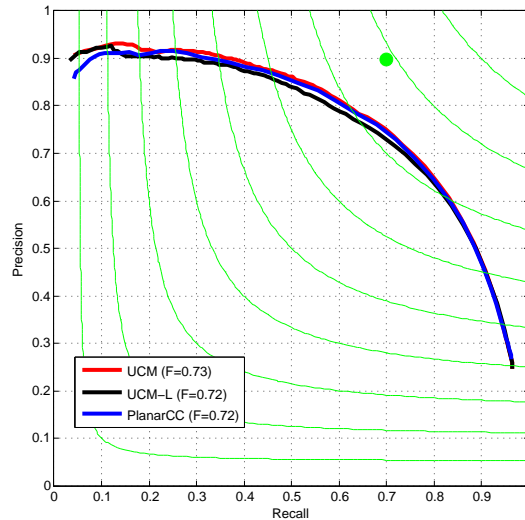


Fig. 3. Evaluation on the BSDS500 segmentation boundary benchmark. We compare segmentation performance to the state of the art technique (gPb+owt+UCM) proposed by [34]. We use the same set of superpixels and contour cues derived from (gPb+owt). We compare to two different variants of the UCM algorithm based on region merging. UCM performs a length weighted average of the gPb along contours after each merge while UCM-L performs a uniform average. We find that the globally optimal correlation clustering returned by our algorithm performs slightly better than the uniform averaging version of UCM but the length-weighted UCM gives better final performance.

two variants of the UCM algorithm. As visible in the figure, our algorithm performs comparably to UCM and performs slightly better than the results of [18] who report an F-measure of 0.70.

The UCM algorithm is a region merging algorithm that successively merges the two superpixels that have the lowest energy edge between them. Since this algorithm is “greedy” with respect to the clustering objective, we would expect that it would occasionally merge two segments due to some small break in the contour contrast, a fate that our global optimization approach could avoid. However, as is clear from Figure 3, in practice the greedy nature of UCM does not seem to significantly hurt overall performance.

One explanation is that the UCM algorithm modifies the edge costs as it proceeds. After each merging step, any new contours that have been formed are re-assigned the average of the underlying gPb . Our global clustering objective cannot capture this length weighted averaging. Figure 3 shows performance of the UCM algorithm with length-weighted averaging (UCM) and simple averaging (UCM-L). While our approach outperforms the non-length weighted version, the differences are not substantial.

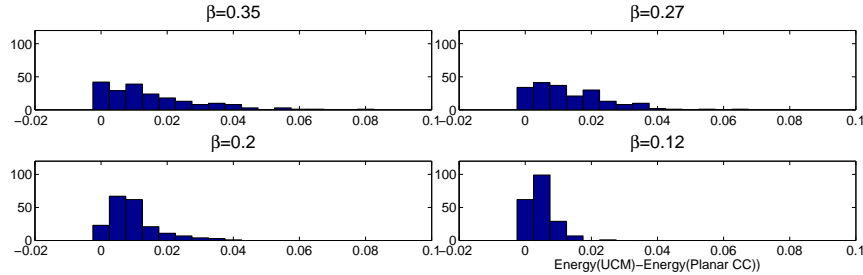


Fig. 4. We find that our algorithm returns lower-energy segmentations than the UCM algorithm. This suggests either a mismatch between the correlation clustering model and the ground-truth or that our model is using suboptimal settings for the local boundary cues

Another possible explanation is that the greedy merging is truly successful in optimizing the correlation clustering objective. Figure 4 shows that this is not the case – while there is usually some UCM threshold that provides a segmentation with a fairly low-cost clustering, it is still suboptimal compared to the solutions returned by PlanarCC. This suggests learning an optimal cue combination via structured prediction may improve performance.

Finally, it is worth noting that the boundary detection benchmark does not provide strong penalties for small leaks between two segments when the total number of boundary pixels involved is small. We found that on the region based benchmarks, PlanarCC did outperform UCM slightly when the optimal segmentation threshold was chosen on a per-image basis (GT Covering OIS 0.65 versus 0.64 for UCM). We expect these differences may become more apparent in an application where the local boundary signal is noisier (e.g., biological imaging) or when there is a greater cost for under-segmentation.

8 Conclusion

We have presented a novel, fast algorithm for finding high quality correlation clusterings in planar graphs. Our algorithm appears to outperform existing approaches on a variety of real problem instances. Our method exploits decomposition into subproblems that lack efficient combinatorial algorithms but are still tractable in the sense having efficient oracles. This offers a new technique in the toolkit of Lagrangian relaxations that we expect will find further use in the application of dual-decomposition to vision problems.

Acknowledgments: This work was supported by a Google Research Award, the UC Lab Fees Research Program and NSF DBI-1053036.

References

1. Boykov, Y., Veksler, O., Zabih, R.: Fast approximate energy minimization via graph cuts. *PAMI* (2001)
2. Borenstein, E., Ullman, S.: Combined top-down/bottom-up segmentation. *PAMI* (2008)
3. Winn, J., Shotton, J.: The layout consistent random field for recognizing and segmenting partially occluded objects. In: *CVPR*. (2006)
4. Levin, A., Weiss, Y.: Learning to combine bottom-up and top-down segmentation. *International Journal of Computer Vision* **81** (2009) 105–118
5. Yang, Y., Hallman, S., Ramanan, D., Fowlkes, C.: Layered object models for image segmentation. *TPAMI* (2011)
6. Gould, S., Gao, T., Koller, D.: Region-based segmentation and object detection. In: *NIPS*. (2009)
7. Ladicky, L., Sturges, P., Alahari, K., Russell, C., Torr, P.: What, where and how many? combining object detectors and crfs. In: *ECCV*. (2010)
8. Shi, J., Malik, J.: Normalized cuts and image segmentation. *PAMI* (2000)
9. Wang, S., Kubota, T., Siskind, J.M., Wang, J.: Salient closed boundary extraction with ratio contour. *PAMI* (2005)
10. Zhu, Q., Song, G., Shi, J.: Untangling cycles for contour grouping. *ICCV* (2007)
11. Sharon, E., Galun, M., Sharon, D., Basri, R., Brandt, A.: Hierarchy and adaptivity in segmenting visual scenes. *Nature* **442** (2006) 810–813
12. Cour, T., Benezit, F., Shi, J.: Spectral segmentation with multiscale graph decomposition. *CVPR* (2005)
13. Taskar, B.: *Learning Structured Prediction Models: A Large Margin Approach*. Stanford University (2004)
14. Bansal, N., Blum, A., Chawla, S.: Correlation clustering. *Machine Learning* **56** (2004) 89–113
15. Demaine, E., Emanuel, D., Fiat, A., Immorlica, N.: Correlation clustering in general weighted graphs. *Theoretical Computer Science* **361** (2006) 172–187
16. Dahlhaus, E., Johnson, D., Papadimitriou, C., Seymour, P., Yannakakis, M.: The complexity of multiterminal cuts. *SIAM J. Computing* **4** (1994) 864–894
17. Bachrach, Y., Kohli, P., Kolmogorov, V., Zadimoghaddam, M.: Optimal coalition structures in graph games. In: *arXiv:1108.5248v1*. (2011)
18. Andres, B., Kappes, J., Beier, T., Koethe, U., Hamprecht, F.: Probabilistic image segmentation with closedness constraints. In: *ICCV*. (2011)
19. Kim, S., Nowozin, S., Kohli, P., Yoo, C.: Higher-order correlation clustering for image segmentation. In: *NIPS*. (2011)
20. Appel, K., Haken, W.: *Every Planar Map is Four-Colorable*. American Mathematical Society (1989)
21. Wainwright, M.J., Jaakkola, T., Willsky, A.S.: MAP estimation via agreement on (hyper)trees: message-passing and linear programming approaches. *IEEE Trans. Inform. Theory* **51** (2005) 3697–3717
22. Kolmogorov, V.: Convergent tree-reweighted message passing for energy minimization. *IEEE Trans. Pattern Anal. Machine Intell.* **28** (2006) 1568–1583
23. Kasteleyn, P.: Graph theory and crystal physics. In Frank Harary, editor, *Graph Theory and Theoretical Physics* (1967) 43–110
24. Fisher, M.: On the dimer solution of planar Ising models. **7(10):1776-1781** (1966)
25. Globerson, A., Jaakkola, T.: Approximate inference using planar graph decomposition. In: *NIPS*. (2007) 473–480

26. Schraudolph, N., Kamenetsky, D.: Efficient exact inference in planar Ising models. In: NIPS. (2009)
27. Schraudolph, N.: Polynomial-time exact inference in np-hard binary MRFs via reweighted perfect matching. In: AISTATS. (2010)
28. Batra, D., Gallagher, A., Parikh, D., Chen, T.: Beyond trees: MRF inference via outer-planar decomposition. In: CVPR. (2010)
29. Yarkony, J., Ihler, A., Fowlkes, C.: Planar cycle covering graphs. In: UAI. (2011)
30. Komodakis, N., Paragios, N., Tziritas, G.: MRF optimization via dual decomposition: Message-passing revisited. In: ICCV, Rio de Janeiro, Brazil (2007)
31. Deza, M., Laurent, M.: Geometry of cuts and metrics. Springer-Verlag (1997)
32. Barahona, F.: The max cut problem in graphs not contractible to K_5 . Operations Research Letters **2** (1983) 107–111
33. Martin, D., Fowlkes, C., Tal, D., Malik, J.: A database of human segmented natural images and its application to evaluating segmentation algorithms and measuring ecological statistics. ICCV (2001)
34. Arbelaez, P., Maire, M., Fowlkes, C., Malik, J.: Contour detection and hierarchical image segmentation. IEEE TPAMI **33** (2011) 898–916
35. Kolmogorov, V.: Blossom V: A new implementation of a minimum cost perfect matching algorithm. Mathematical Programming Computation **1(1)** (2009) 43–67
36. Schraudolph, N., Kamenetsky, D.: Efficient exact inference in planar Ising models. Technical Report 0810.4401 (2008)
37. Sontag, D., Meltzer, T., Globerson, A., Weiss, Y., Jaakkola, T.: Tightening LP relaxations for MAP using message passing. In: UAI. (2008)
38. Sontag, D., Jaakkola, T.: New outer bounds on the marginal polytope. In: NIPS. (2007)
39. Barahona, F., Mahjoub, A.: On the cut polytope. Mathematical Programming **36** (1986) 157–173
40. Yarkony, J.: Planarity Matters: MAP inference in Planar Markov Random Fields with Applications to Computer Vision. University of California, Irvine (2012)

Appendix A: Derivation of the LP dual

It is informative to analyze the dual LP to the bound optimization presented in Equation (14) of the paper:

$$\begin{aligned}
& \max_{\lambda} \sum_e (\theta_e - \lambda_e) & (17) \\
& \text{s.t. } \theta_e \leq \lambda_e \leq \max\{0, \theta_e\} \\
& \sum_e \lambda_e X_e \geq 0 \quad \forall X \in \mathcal{C}_2
\end{aligned}$$

In order to write this in a standard form, define

$$\tilde{\lambda}_e = \lambda_e - \theta_e$$

and

$$\tilde{\theta}_e = \max(0, \theta_e) - \theta_e = -\min(0, \theta_e)$$

Let C be a matrix whose rows are the collection of cut indicator vectors X . Let us assume for now that C contains the entire set of cut vectors. We can write the LP in standard form:

$$\begin{aligned}
& \max_{\tilde{\lambda}} -1^T \tilde{\lambda} & (18) \\
& \text{s.t. } \tilde{\lambda} \geq 0 \\
& \tilde{\lambda} \leq \tilde{\theta} \\
& -C\tilde{\lambda} \leq C\theta
\end{aligned}$$

which has the following dual LP:

$$\begin{aligned}
& \min_{\alpha, \beta} \theta^T C^T \alpha + \tilde{\theta}^T \beta & (19) \\
& \text{s.t. } \alpha \geq 0 \\
& \beta \geq \max(0, C^T \alpha - 1)
\end{aligned}$$

To further simplify the expression, we define the set $\mathcal{C}_2^\Delta = \{C^T \alpha, \alpha \geq 0\}$ which is the convex cone known as the ‘‘cut cone’’ [31]. Since $\tilde{\theta} \geq 0$, β will always take on its minimum allowable value so we can collapse it into the objective, yielding:

$$\begin{aligned}
& \min_z \theta^T z - \min(\theta^T, 0) \max(z - 1, 0) & (20) \\
& \text{s.t. } z \in \mathcal{C}_2^\Delta
\end{aligned}$$

Observe that the second term in the objective is 0 when $z \leq 1$ and is positive when $z > 1$.

If we drop the upper-bound constraints on λ in Equation (14) in the main paper, we get the simplified dual LP:

$$\begin{aligned} \min_z \quad & \theta^T z \\ \text{s.t.} \quad & z \in \mathcal{C}_2^\Delta \\ & z \leq 1 \end{aligned} \tag{21}$$

As discussed in the paper, this analysis provides several insights on the nature of the lower-bound:

1. One can see that geometrically, the PlanarCC bound is equivalent to optimizing over a relaxation of the multi-cut polytope given by the intersection of the cut cone and the unit hypercube. This seems natural since the cut cone and the multi-cut cone coincide [31] and the cut cone can be compactly described for planar graphs.
2. Intuitively, the upper-bound constraints on λ in the original LP are irrelevant to the final value of the LP in the case that all cuts are included in C . This is because any multicut can be represented as a sum of isolating cuts, each with weight 0.5. If such a solution optimizes LP (5), it is also optimal for LP (4). We give a detailed proof in the next section which holds even when C only includes a subset of cuts.
3. Finally, one can see the relation between this bound and the standard cutting plane approaches used, for example, in [38] or the ILP solution of [18]. In a standard cutting-plane approach, one optimizes the LP relaxation $\min \theta^T z$ with a subset of the constraints that define the multi-cut polytope and then successively add constraints, carving away parts of the search space until an integral solution is found. In contrast, each time we add a cutting plane to our primal LP, this adds another row to the matrix C in the dual LP which expands the set of allowable solutions z . Thus our algorithm can be viewed as a delayed column generation scheme for the dual LP in which we keep growing the space of reachable z until an optimum is found.

Appendix B: Additional constraints on λ don't affect the bound

In Section 5 we introduced the constraint $\lambda_e \leq \max\{0, \theta_e\}$ without a formal justification. Here we show this constraint does not decrease the lower-bound. Suppose we first optimize the lower-bound without including the constraint $\lambda_e \leq \max\{0, \theta_e\}$. Let λ^* denote the optimizing parameters. Our strategy is to show that λ^* can be modified to satisfy $\lambda_e \leq \max\{0, \theta_e\} \forall e$ without loosening the bound.

We first restate the definition of the lower-bound:

$$CC^* \geq \sum_e (\theta_e - \lambda_e^*) + \min_{X \in \mathcal{C}_2} \sum_e \lambda_e^* X_e \tag{22}$$

The convex hull of the set of cut indicator vectors is known as the cut polytope [31] which we denote \mathcal{C}_2^\square . For planar graphs, this polytope is compactly described by the set of cycle inequalities [39]. One can relax the discrete optimization over \mathcal{C}_2 to an LP over the cut polytope (see e.g., [38]). In the following analysis, we work with the dual of this relaxed LP in which we have a collection of dual variables $\{\phi_e^c\}$ corresponding to the constraint on each cycle c of the planar graph [40].

$$\min_{X \in \mathcal{C}_2^\square} \sum_e \lambda_e^* X_e = \max_{\phi: \sum_c \phi_e^c = \lambda_e^*} \sum_c \min_{X^c \in \mathcal{C}_2} \sum_e \phi_e^c X_e^c \quad (23)$$

The right-hand side corresponds to dual-decomposition into a collection of sub-problems, each of which is a cycle from the original graph. Let ϕ^* denote an optimizer of this dual LP. We write our lower-bound in terms of this cycle decomposition as:

$$CC^* \geq \sum_e (\theta_e - \lambda_e^*) + \sum_c \min_{X^c \in \mathcal{C}_2} \sum_e \phi_e^{*c} X_e^c \quad (24)$$

Lemma 1: For all cycles c , $\min_{X^c \in \mathcal{C}_2} \sum_e \phi_e^{*c} X_e^c = 0$.

Lemma 1 holds because the minimum energy of each subproblem for a cycle c is upper-bounded by zero and the sum of all the cycle subproblem energies is zero due to the constraint $\lambda^* \in \Omega$. Notice that if there is a negative valued parameter ϕ_e^{*c} on the c 'th cycle sub-problem then any other edge $f \neq e$ must have a parameter setting such that $\phi_e^{*c} + \phi_f^{*c} \geq 0$. Otherwise, the configuration which cuts e and f would have negative energy. In particular, this implies that each cycle subproblem can only have a single negative parameter.

Lemma 2: For each edge e with $(\theta_e - \lambda_e^* < 0)$ contained in a cycle c , either $(\phi_e^{*c} < 0)$ or $(\exists f \text{ s.t. } \phi_e^{*c} + \phi_f^{*c} = 0)$.

Suppose there existed an edge e and cycle c for which the implication of the lemma is false, that is $(\theta_e - \lambda_e^* < 0)$, $(\phi_e^{*c} \geq 0)$ and $(\forall f : \phi_e^{*c} + \phi_f^{*c} > 0)$. This would mean there is no minimizing configuration of the cycle subproblem that includes edge e (such a cut would have positive weight). However, edge e is necessarily cut in the single edge problem. In such a case the lower-bound could be tightened by the following update:

$$\begin{aligned} f &= \arg \min_{f \neq e} (\phi_e^{*c} + \phi_f^{*c}). \\ V &= \min[-(\theta_e - \lambda_e^*), \phi_e^{*c} + \phi_f^{*c}] \\ \lambda_e^* &\Leftarrow \lambda_e^* - V \\ \phi_e^{*c} &\Leftarrow \phi_e^{*c} - V \end{aligned} \quad (25)$$

This update would drive up the energy of the single edge problem thus increasing the lower-bound by a positive quantity V . Since the lower-bound is tight by

assumption, such an edge e and cycle c must not exist.

Modifying λ to satisfy the constraint: We now describe an iterative procedure that starts with λ^* and ϕ^* and produces a modified λ^+ and ϕ^+ obeying the constraint:

$$(\theta_e - \lambda_e^+ < 0) \rightarrow (\phi_e^{+c} \leq 0) \quad \forall [c, e] \quad (26)$$

The lower-bound corresponding to λ^+ will have the same value as that of λ^* and will satisfy the additional upper-bound constraint as desired.

For each (e, c) such that $(\theta_e - \lambda_e^* < 0)$ and $(\phi_e^{*c} > 0)$, Lemma 2 establishes that there exists an edge f so that $(\phi_e^{*c} + \phi_f^{*c} = 0)$. Choose one such edge f and apply the parameter updates:

$$\begin{aligned} V &\Leftarrow \max[\theta_e - \lambda_e^*, -\phi_e^{*c}] & (27) \\ \phi_e^{*c} &\Leftarrow \phi_e^{*c} + V \\ \phi_f^{*c} &\Leftarrow \phi_f^{*c} - V \\ \lambda_e^* &\Leftarrow \lambda_e^* + V \\ \lambda_f^* &\Leftarrow \lambda_f^* - V \end{aligned}$$

Repeatedly apply these updates until there exist no (e, c) such that $(\theta_e - \lambda_e^* < 0)$ and $(\phi_e^{*c} > 0)$. These updates do not change the minimizing configuration or energy of either the cycle or edge subproblems. They also respect the lower-bound constraint $\theta_e \leq \lambda_e$. Thus the bound remains constant. The final results of this procedure are denoted λ^+ and ϕ^+ .

Lemma 3: For all edges e , $(\theta_e - \lambda_e^+ < 0) \rightarrow (\lambda_e^+ \leq 0)$

The algorithm terminates when $(\theta_e - \lambda_e^+ < 0) \rightarrow (\phi_e^{+c} \leq 0)$ for all cycles c and edges e . Since ϕ^+ is a reparameterization of λ^+ we have that $\sum_c \phi_e^{+c} = \lambda_e^+$ for each edge e which establishes the lemma.

Claim: For all edges e , $\lambda_e^+ \leq \max\{0, \theta_e\}$

If $(\theta_e - \lambda_e^+ = 0)$ then the claim is satisfied. If $(\theta_e - \lambda_e^+ < 0)$ then by Lemma 3 we have $(\lambda_e^+ \leq 0)$. For such an edge, it must be that $\theta_e < 0$ as we can't simultaneously have $(\theta_e - \lambda_e^+ < 0)$, $\lambda_e^+ \leq 0$ and $\theta_e \geq 0$. Thus, we can transform any optimizer λ^* into an optimizer λ^+ that achieves the same lower-bound and satisfies the additional constraints.